Preprints (www.preprints.org) | NOT PEER-REVIEWED | Posted: 7 August 2020 doi:10.20944/preprints202008.0192.v1

Monitoring five years of the whiting phenomenon in the Gitana lake (Cuenca, Spain) using Sentinel-2 images

M. Ruiz; S. Morales; J.M. Soria*
* Corresponding author email: juan.soria@uv.es
Department of Microbiology & Ecology, Faculty of Biological Sciences, University of Valencia. 46100 – Burjassot, Spain

Abstract

In the present study, a five-year follow-up was performed by remote sensing of the calcium carbonate precipitation in La Gitana karstic lake (located on the province of Cuenca, Spain). The important role that calcium carbonate precipitation plays in the ecology of the lake is well known for its influence on the vertical migrations of phytoplankton, the concentration of bioavailable phosphorus and, therefore, the eutrophication and quality of the waters. Whiting take place between the months of July and August, and it can be studied at this time through its optical properties, with the main objective of offering updated data on a phenomenon traditionally studied and establishing possible relationships between abiotic factors such as temperature and/or rainfall. The atmospheric temperature data collected by the meteorological station suggest a possible relationship between the appearance of the white phenomenon and a pulse of previous maximum temperatures. On the other hand, no apparent relationship was found between rainfall and water bleaching.

Keywords: calcium carbonate, karst, precipitation, remote sensing, whiting

1. Introduction

Inland surface waters form valuable ecosystems (Buchanan and Stubblebine, 1962) of great importance for global biodiversity (Wunder, 2015). Globally, there are more than 100 million lakes (Verpoorter *et al.*, 2014) that support up to 87% of the world's freshwater. (Gleick, 1993). These natural resources are particularly sensitive to climate change, so variables such as lake surface temperature, water level and lake color are characterized as Essential Climate Variables (ECVs), thus recognized by the Global Climate Observing System (GCOS) as contributing critically to the characterization of climate change. (Woolway *et al.*, 2020).

Karst lakes are lenitic ecosystems, with waters more or less rich in bicarbonates (Camacho *et al.*, 2009), which develop on sedimentary rocks, mainly calcium (limestone), magnesium (dolomite), carbonates, but also calcium sulphate minerals (gypsum) (Casamayor *et al.*, 2012). Because they are associated with areas where karstification phenomena are very active (Camacho *et al.*, 2009), these types of lakes frequently have rounded shapes, steep sides, no surface entrances or exits and a relatively high depth. Therefore, the waters are often thermally stratified, giving rise to

© 2020 by the author(s). Distributed under a Creative Commons CC BY license.

Preprints (www.preprints.org) | NOT PEER-REVIEWED | Posted: 7 August 2020 doi:10.20944/preprints202008.0192.v1

water compartments with different physicochemical and biological conditions. (Casamayor *et al*., 2012).

Due to the oligotrophic characteristics of the waters, they allow the development of communities dominated by charophytes. This type of ecosystems are catalogued and named as: "3140 Oligomesotrophic calcareous waters with benthic vegetation of *Chara* spp" by the Habitats Directive 92/43CEE of Annex 1 (Camacho *et al*., 2009). Underwater meadows of *Chara* spp. are a good bio-indicator of water quality as their populations decline when water eutrophy increases. (Cirujano *et al*., 2007).

The Cruz Lake, or Gitana Lake, is the water body on which this study is based. It has an approximate surface area of 1.4 ha, an average diameter of 132 m and a maximum depth of 25 m (CMADR, 2007). Considering all the karstic area in the mountains of Cuenca, only two lenitic systems (Cruz Lake and El Tobar Lake) of 35 have meromictic characteristics. (Miracle *et al*., 1992). Laguna de la Cruz presents a biogenic meromixis, due to the enrichment of the monimolimnion water (the deep layer not mixed without any exchange with the upper waters, except for slow diffusion processes (Izhitskiy *et al*., 2016)) in calcium, magnesium, and iron bicarbonates (Miracle *et al*., 1992). These physicochemical changes are evident every summer, at the end of July, when the blue-green waters of the lake acquire a milky appearance due to calcium carbonate precipitation (CMADR, 2007) favoured by high temperatures, high pH and/or an increase in primary production. (Vanderploeg *et al*., 1987; Homa and Chapra, 2011).

The aim of the work is to carry out a short- and long-term monitoring of the whiting phenomenon of the karstic lake of Cañada del Hoyo through a thematic analysis of the optical properties of the lagoon using Sentinel-2 satellite images. In this way, it is possible to collect updated data on the whiting phenomenon of the Gitana lake, dates when it starts and check its duration in time.

2. Materials and methods

2.1. Context, Cañada del Hoyo karstic lakes

The present study is developed on the site known as “Lagunas de Cañada del Hoyo”, catalogued as a natural monument in 2007. They are located southeast of Los Palancares, in the karst area called Los Oteros, in the central-eastern part of the province of Cuenca (Spain). It consists of a group of dolines, seven of which maintain water permanently and are known as: Cruz or Gitana, Tejo, Lagunillo, Parra, Llana, Tortugas and Cardenillas. (CMADR, 2007).

Preprints (www.preprints.org) | NOT PEER-REVIEWED | Posted: 7 August 2020 doi:10.20944/preprints202008.0192.v1

Figure 1. Location of the Cañada del Hoyo karstic complex in the Iberian Peninsula. The seven lakes are highlighted in a circle with their respective names near. Next to them there are other dolines with no water at the bottom (Source: modified from Google Earth).

2.2. Monitoring the phenomenon

The monitoring of the "whiting phenomenon", as the exclusive optical property of the Gitana lake, was carried out through the use of satellite images from the Sentinel-2 platform of the European Space Agency, obtained from the Copernicus Open Access Hub repository and subsequently processed with the SNAP satellite image processing software.

The Copernicus download platform holds images from the start of Sentinel-2 operation in 2015 to the present day. Therefore, the monitoring of the whiting phenomenon runs from the summer of 2015 to the summer of 2019, between the beginning of July and the end of August, as these are the dates when the whiting phenomenon occurs.

The images were downloaded with level 1 processing (L1C). Atmospheric correction was performed by means of the C2RCC SNAP module using C2X as the methodology. The images were resampled and cropped (10 m pixel resolution) using the geographic coordinates as the boundary area 40.00 N; -1.90 W; 39.97 N; -1.85 W. Bands 2, 3 and 4 were selected to display in false color (RGB) the white phenomenon.

At the same time, data on atmospheric temperature and rainfall were collected at the Cuenca weather station during the dates covered by the study period.

3. Results

A total of 59 Sentinel-2 images have been downloaded through the Copernicus Open Access Hub (see the list of downloaded images and their corresponding dates in the table in Annex A1). A first visual observation has been made (figure 2), as changes within the visible spectrum clearly indicate the absence or presence of the whiting phenomenon in the Gitana lake (figure 3). It can be seen how the increase in reflectivity in the blue and green bands is remarkable with respect to the normal image.

Preprints (www.preprints.org) | NOT PEER-REVIEWED | Posted: 7 August 2020 doi:10.20944/preprints202008.0192.v1

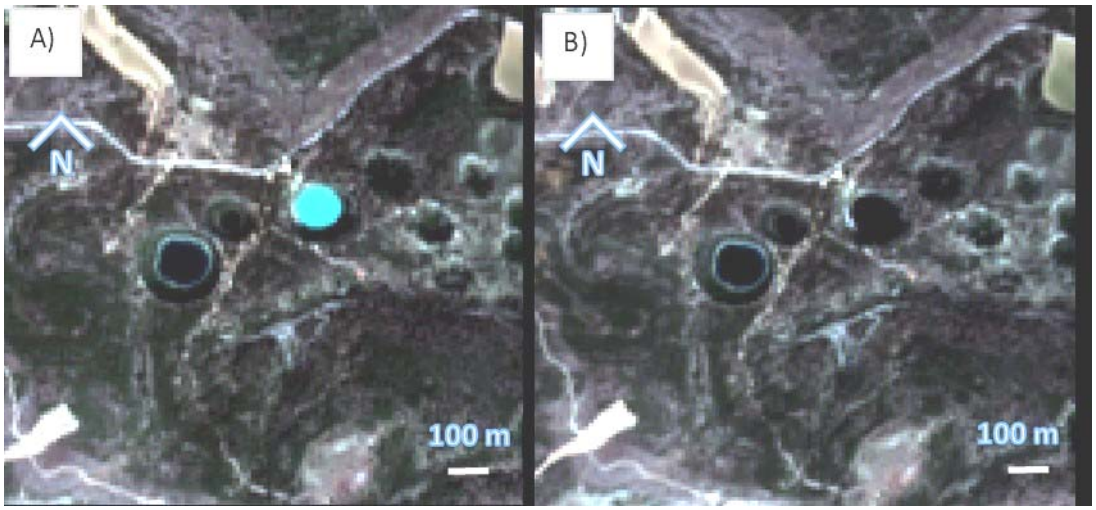

Figure 2. Comparison of optical properties of the Gitana lake in false colour: A) the view on Aug 22, 2018 during the whiting phenomenon and B) the lagoon on July 20, 2018 in its normal state (view in false colour RGB from bands 2, 3 and 4).

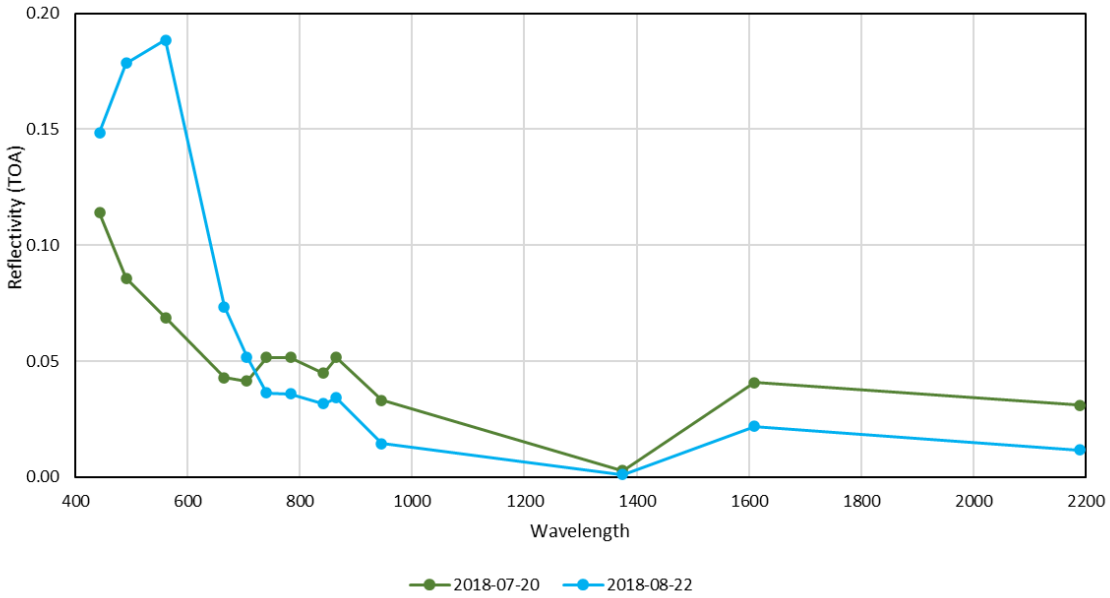

Figure 3. Comparison of the radiometric spectrum TOA (top of atmosphere) of the Gitana Lake in the presence of the whiting phenomenon (blue libe, image of Aug 22, 2018) and in the absence of the whiting phenomenon (green line, image of July 20, 2018).

On the other hand, band 8, which covers the near-infrared spectral region, has been used as an indicator of the surface of the lagoon.

In the five years studied, the year 2015, the whiting phenomenon could only be observed in one image in the Sentinel-2 images, on July 16; moreover, this was the earliest date of the year in which it appeared. In 2016, the whiting phenomenon was observed in three images over an 11-day period between August 9 and 19. In 2017, the whiting phenomenon was observed in four images from July 25 to August 7, 14 days in total. In 2018, the whiting phenomenon was recorded with the latest onset, from August

Preprints (www.preprints.org) | NOT PEER-REVIEWED | Posted: 7 August 2020 doi:10.20944/preprints202008.0192.v1

22 to September 1 (a total of 11 days) and was observed in five images. In 2019, the whiting was first observed in the images of August 9 and the disappearance on August 19 in the Gitana lake, in total in four images. For each year, the figure has been made with a false colour image of the lagoon in its normal state and with the whiting, which are presented in Annex 2.

Meteorological data have also been obtained for the months of July and August in order to study the relationships between recorded temperatures and rainfall and the whiting of the water. The temperature data for the five years, as well as the precipitation data, are presented in the tables in annex 1. Figure 4 shows, for the five years studied, the evolution of the maximum temperature observed and the dates of observation of the phenomenon.

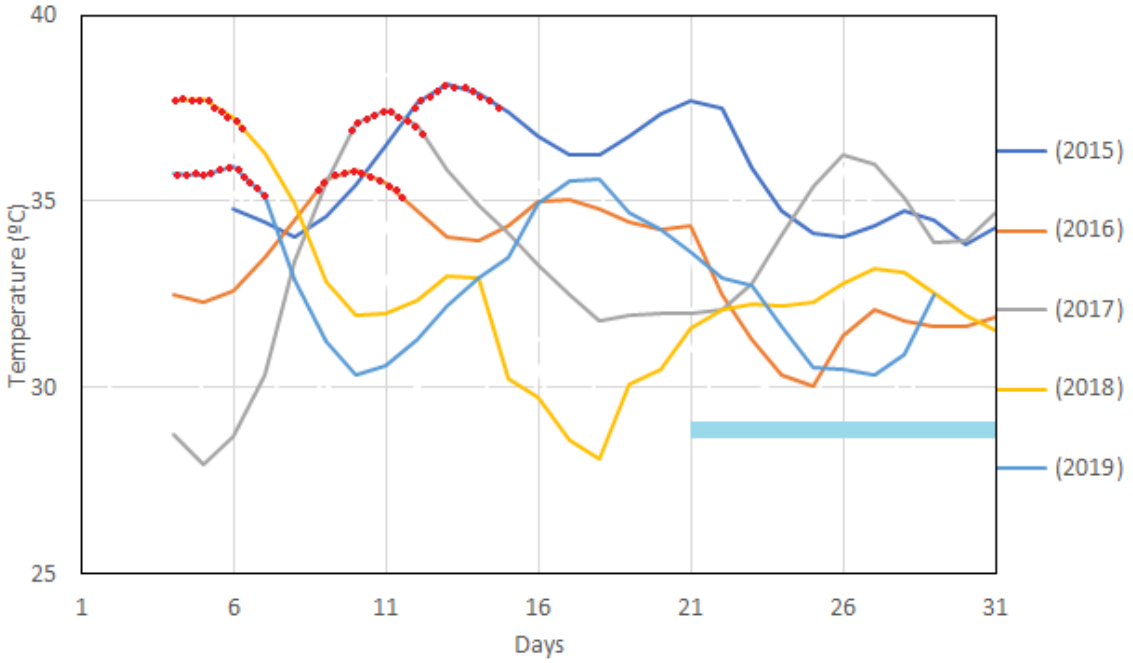

Figure 4. Four-day moving average of temperature in the period studied each year. On the 21st day of each year is the first observation of whiting and its duration is placed with a blue band. The dashed red line indicates the period of maximum recorded temperature.

The appearance of the whiting is sudden and is observed in only three days, as is the case in the year 2016, where it begins on August 9 and is total on August 12. It can be seen how the start coincides with very high maximum temperatures some twelve days before (figure 4). In the case of 2018, where the process was the latest, these higher temperature values took place fourteen days earlier. In 2016 and 2017 they took place twelve and eleven days earlier. In 2015 the maximum temperatures were eight days earlier and in 2019 they were also fourteen days earlier. It is true that we are in the month of July and August and these are the periods of maximum temperatures of the year in this region.

The decay of the white phenomenon is slower and takes a few days longer, as it is a process of sedimentation of particulate matter. In the case of the year 2019, the

Preprints (www.preprints.org) | NOT PEER-REVIEWED | Posted: 7 August 2020 doi:10.20944/preprints202008.0192.v1

meteorological conditions allowed us to have all the satellite images of the days of the phenomenon and this sequence can be seen perfectly in figure 5. It can be seen that on August 4 there is no phenomenon or in any case it is in its early stages, on August 9 the whitening is complete and on August 12 it continues; but on the 14th it already declines and on the 17th it is already a blue-green colour, on August 19 it is almost normal.

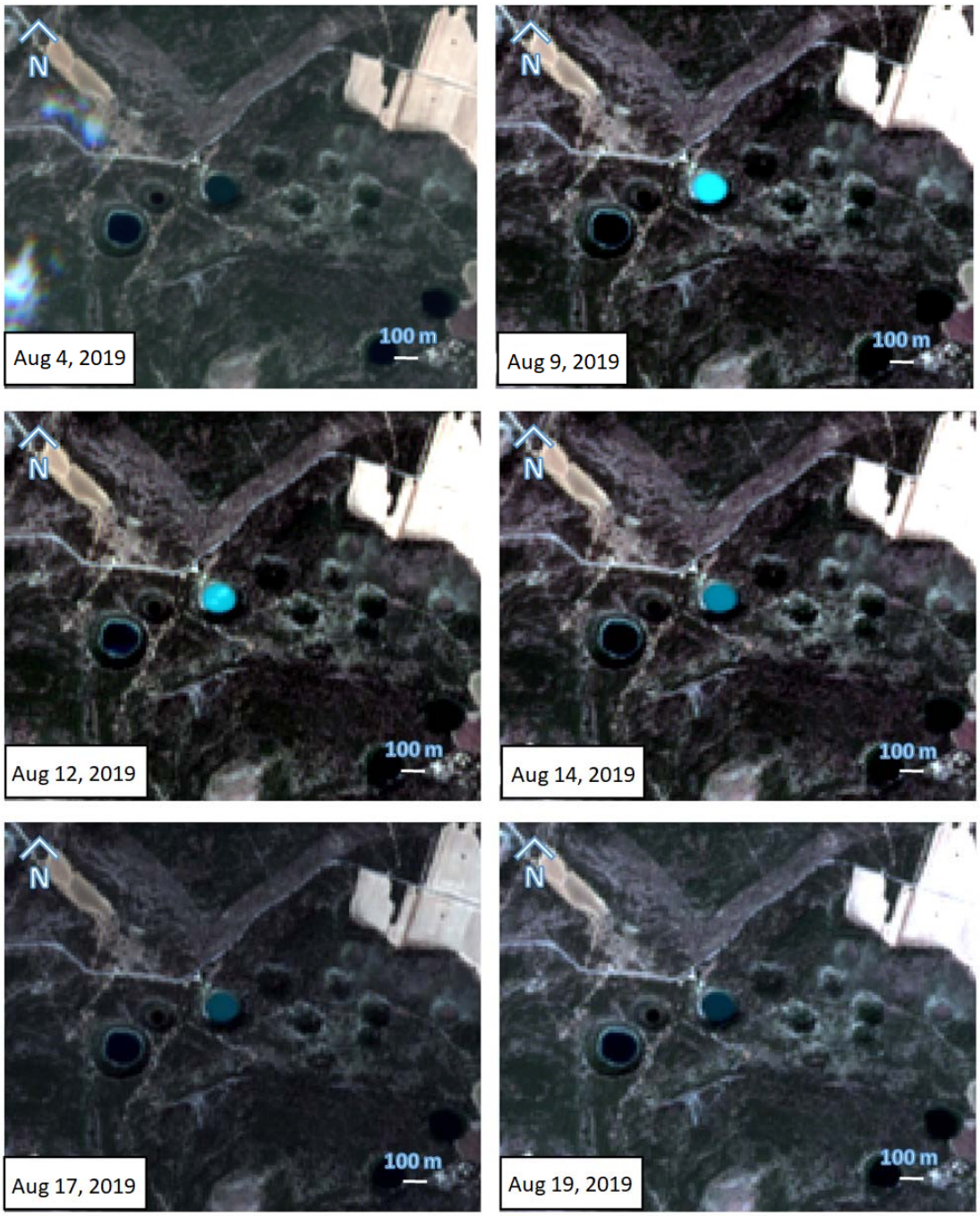

Figure 5. Observation of the whiting phenomenon between August 4 and 19, 2019 (RGB false colour processing from Sentinel-2 images).

4. Discussion

Through the processing of satellite images, it has been possible to monitor the annual phenomenon of the whitening of the Gitana lake on an annual and almost daily basis in

Preprints (www.preprints.org) | NOT PEER-REVIEWED | Posted: 7 August 2020 doi:10.20944/preprints202008.0192.v1

search of any kind of irregularities or new data that could guide future linmological studies to find out in more detail what exactly are the triggers of the white phenomenon since, to date, numerous investigations point in similar directions but these data are not sufficient to make exact predictions of when the next event of whitening of the lagoon will take place. The availability of the combined Sentinel-2A and 2B high frequency images allows up to five images of the phenomenon as in 2019, when in 2015 only one image was observed.

4.1. Duration of the phenomenon.

In the five years studied, the white phenomenon has not appeared more than once per year. Nor is it mentioned in the work carried out since 1980 on the Gitana lake that there have ever been two periods. This should indicate that the whitening of the lagoon is on an annual cycle.

A remarkable fact is the length of time the lagoon remains white. In the table Annex A1 shows that in these years, the phenomenon lasts at least approximately one week (Miracle *et al*., 1992; Rodrigo *et al*., 1993) and the maximum would be 18 days, considering that Sentinel-2 images have been collected every three to five days. It is important to note that the lack of satellite images available for some years makes it difficult to count the exact days when the lagoon presents the phenomenon as in 2015.

According to Rodrigo *et al*. (1993), by comparison with other lagoons that also present a calcium carbonate precipitation phenomenon, the Gitana lake has the shortest water bleaching period. This short period of approximately 15 days contrasts with processes that take months, such as in the case of Lake Powell, located between Arizona and Utah, which has a six-month bleaching process (Reynolds, 1978), two months in Lake Michigan (Strong and Eadie, 1978), one month in Lake Pyramid, in Nevada (Galat and Jacobsen, 1985) and, as an extreme case, Lake Balaton, which remains like this throughout the year (Dobolyi and Herodek, 1980).

4.2. Beginning of the white phenomenon

The results obtained indicate that there is no exact date of onset of the phenomenon, it can only be limited to the months of July and August (and exceptionally to the beginning of September); more specifically, during the last week of July or the first week of August (Miracle *et al*., 1992) being the hottest period of the year. This may indicate that the white phenomenon requires high temperatures to be triggered directly or indirectly.

It is known that the processes of carbonate mineralization in lakes and lagoons depend to a great extent on a series of geochemical and biological factors. (Reddy, 1995).

According to Miracle *et al*. (1992) high temperatures favor $CaCO_3$ saturation, thus triggering precipitation and whiting. In addition, there are prokaryotic organisms that, due to their metabolic activity, can trigger the bioprecipitation of calcium carbonate in the aquatic environment they inhabit (Seifan and Berenjian, 2019) but the effectiveness of this process depends largely on abiotic factors such as the concentration of dissolved inorganic carbon, nucleation point, pH, temperature and redox potential (Eh) (Barton and Northup, 2011; Hammes and Verstraete, 2002). Studies by Müller *et al*. (2016) on

Preprints (www.preprints.org) | NOT PEER-REVIEWED | Posted: 7 August 2020 doi:10.20944/preprints202008.0192.v1

biogenic precipitation of calcium carbonate in lakes also attribute this phenomenon to an increase in pH caused by algae growth and by the nucleation of calcite crystals on the surface of microalgae.

In this study, the atmospheric temperature data collected by the Cuenca weather station indicate, although vaguely, a possible relationship between the white phenomenon and a previous pulse of maximum temperatures close to 40 ºC (figure 4). The proof is that in 2018 the start of the phenomenon was delayed until the end of August, as the maximum temperatures were not reached in July. On the other hand, the precipitation data does not seem to be an important factor in the beginning of the target phenomenon, as well as the relation with the reflectivity of the 8 NIR band used in this study as a possible indicator of the water temperature of the Gitana lake.

Studies on this phenomenon offer great contributions to the branch of ecology, limnology and geology since the whitening of the waters has an important role in the ecology of the lake. Traditionally, the precipitation reaction of calcium carbonate is considered to serve as a buffer against eutrophication of karstic lakes (Kleiner, 1988; Robertson *et al*., 2007; Hamilton *et al*., 2009). Phosphorus (P) is incorporated by coprecipitation into the calcium carbonate crystals, thus reducing the bioavailable P and with it, the abundance of phytoplankton, and the formation of crystals on the phytoplankton induces sinking and senescence. (Stabel, 1986; Koschel, 1987; Mullins, 1998).

For all these reasons, lenitic systems that periodically present calcium carbonate precipitation phenomena are commonly associated with transparent waters that are low in nutrients (Wiik, 2014). In addition to buffering eutrophication, the white phenomenon plays an important role in the vertical migration of phototrophic organisms by significantly decreasing the penetration of light (Rodrigo *et al*., 1993).

By means of remote sensing, it is possible to carry out these detailed follow ups of almost any type of natural phenomenon, as long as it can be investigated through its optical properties (as the cyan colour of the Gitana lake indicates the presence of the whiting phenomenon, figure 5). Studies of natural phenomena by remote sensing do not require high travel costs to the area of study and heavy or expensive laboratory equipment, as it simply requires desk work. Future lines of research will focus on the study of water surface temperature and trophic status from the reflectivity of photosynthetic pigments, as well as on the revision of the Landsat-5 and Landsat-8 archive to have a much longer study period.

5. Conclusions

The use of the SNAP tool as the processing software for Sentinel 2 satellite images and the processing of satellite images resulted in a relatively simple and efficient desktop work, since, in spite of presenting a multitude of different applications, its interface is intuitive and hardly generated any problems or doubts during its use. The availability of Copernicus' images is an essential factor for research work of this type, which combines remote sensing and limnology. The results obtained show the usefulness of the application to a practical case of basic science somewhere between geochemistry and ecology, which is very difficult to do under field conditions. It is important to promote

Preprints (www.preprints.org) | NOT PEER-REVIEWED | Posted: 7 August 2020 doi:10.20944/preprints202008.0192.v1

the use of remote sensing applications in future studies for the monitoring of natural phenomena or for any other reason since the results in the field of research are conclusive with other field works.

References

Barton, L. L., & Northup, D. E., 2011. Microbes at work in nature: biomineralization and microbial weathering. *Microbial Ecology*, 299-326.

Buchanan, J. M., & Stubblebine, W. C., 1962. Externality. *Economica*, 29(116), 138-154.

Camacho, A., Borja, C., Valero-Garcés, B., Sahuquillo, M., Cirujano, S., Soria, J. M., Rico, E., De La Hera, A., Santamans, A. C., García De Domingo, A., Chicote, A. & Gosálvez, R., 2009. 3140 Aguas oligo-mesotróficas calcáreas con vegetación de Chara spp. En: VV.AA., Bases ecológicas preliminares para la conservación de los tipos de hábitat de interés comunitario en España. Madrid: Ministerio de Medio Ambiente, y Medio Rural y Marino. 47 p.

Casamayor, E. O., Llirós, M., Picazo, A., Barberán, A., Borrego, C. M., & Camacho, A., 2012. Contribution of deep dark fixation processes to overall CO_2 incorporation and large vertical changes of microbial populations in stratified karstic lakes. *Aquatic Sciences*, 74(1), 61-75. DOI: 10.1007/s00027-011-0196-5

Cirujano, S., García Murillo, P., & Meco Molina, A., 2007. Los carófitos ibéricos. *Anales del Jardín Botánico de Madrid*, 64(1), 87-102.

Consejería de Medio Ambiente y Desarrollo Rural (CMADR), 2007. Plan de Ordenación de los Recursos Naturales de las Lagunas de Cañada del Hoyo. *D. O. C. M.* Núm. 63

Dobolyi, E., & Herodek, S., 1980. On the mechanism reducing the phosphate concentration in the water of Lake Balaton. *Internationale Revue der gesamten Hydrobiologie und Hydrographie*, 65(3), 339-343. DOI: 10.1002/iroh.19800650303

Galat, D. L., & Jacobsen, R. L., 1985. Recurrent aragonite precipitation in saline-alkaline Pyramid Lake, Nevada. *Archiv für Hydrobiologie*, 105(2), 137-159.

Hamilton, S. K., Bruesewitz, D. A., Horst, G. P., Weed, D. B., & Sarnelle, O., 2009. Biogenic calcite–phosphorus precipitation as a negative feedback to lake eutrophication. *Canadian Journal of Fisheries and Aquatic Sciences*, 66(2), 343-350. DOI: 10.1139/F09-003

Preprints (www.preprints.org) | NOT PEER-REVIEWED | Posted: 7 August 2020 doi:10.20944/preprints202008.0192.v1

Hammes, F., & Verstraete, W., 2002. Key roles of pH and calcium metabolism in microbial carbonate precipitation. *Reviews in environmental science and biotechnology*, 1(1), 3-7.

Homa, E. S., & Chapra, S. C., 2011. Modeling the impacts of calcite precipitation on the epilimnion of an ultraoligotrophic, hard-water lake. *Ecological modelling*, 222(1), 76-90. DOI: 10.1016/j.ecolmodel.2010.09.011

Izhitskiy, A. S., Zavialov, P. O., Sapozhnikov, P. V., Kirillin, G. B., Grossart, H. P., Kalinina, O. Y., Zalota, A. K., Goncharenko, I. V., & Kurbaniyazov, A. K., 2016. Present state of the Aral Sea: diverging physical and biological characteristics of the residual basins. *Scientific reports*, 6(1), 1-9. DOI: 10.1038/srep23906

Kleiner, J., 1988. Coprecipitation of phosphate with calcite in lake water: a laboratory experiment modelling phosphorus removal with calcite in Lake Constance. *Water Research*, 22(10), 1259-1265. DOI: 10.1016/0043-1354(88)90113-3

Koschel, R., Benndorf, J., Proft, G., & Recknagel, F., 1987. Model-assisted evaluation of alternative hypotheses to explain the self-protection mechanism of lakes due to calcite precipitation. *Ecological Modelling*, 39(1-2), 59-65. DOI: 10.1016/0304-3800(87)90013-5

Miracle, M. R., Vicente, E., & Pedrós-Alió, C., 1992. Biological studies of Spanish meromictic and stratified karstic lakes. *Limnetica*, 8, 59-77.

Müller, B., Meyer, J. S., & Gächter, R., 2016. Alkalinity regulation in calcium carbonate-buffered lakes. *Limnology and Oceanography*, 61(1), 341-352. DOI: 10.1002/lno.10213

Mullins, H. T., 1998. Environmental change controls of lacustrine carbonate, Cayuga Lake, New York. *Geology*, 26(5), 443-446. DOI: 10.1130/0091-7613(1998)026<0443:ECCOLC>2.3.CO;2

Reddy, M. M., 1995. *Carbonate precipitation in Pyramid Lake, Nevada. In Mineral Scale Formation and Inhibition*. Boston: Springer.

Reynolds Jr, R. C., 1978. Polyphenol inhibition of calcite precipitation in Lake Powell 1. *Limnology and Oceanography*, 23(4), 585-597. DOI: 10.4319/lo.1978.23.4.0585

Robertson, D.M., Garn, H.S. & Rose, W.J., 2007. Response of calcareous Nagawicka Lake, Wisconsin, to changes in phosphorus loading. *Lake and Reservoir Management* 23(3),298-312. DOI: 10.1080/07438140709354018

Preprints (www.preprints.org) | NOT PEER-REVIEWED | Posted: 7 August 2020 doi:10.20944/preprints202008.0192.v1

Rodrigo, M. A., Vicente, E., & Miracle, M. R., 1993. Short-term calcite precipitation in the karstic meromictic Lake La Cruz (Cuenca, Spain). *Internationale Vereinigung für theoretische und angewandte Limnologie: Verhandlungen*, 25(2), 711-719. DOI: 10.1080/03680770.1992.11900231

Seifan, M., & Berenjian, A., 2019. Microbially induced calcium carbonate precipitation: a widespread phenomenon in the biological world. *Applied microbiology and biotechnology*, 103(12), 4693-4708.

Stabel, H. H., 1986. Calcite precipitation in Lake Constance: Chemical equilibrium, sedimentation, and nucleation by algae 1. *Limnology and Oceanography*, 31(5), 1081-1094. DOI: 10.4319/lo.1986.31.5.1081

Strong, A. E., & Eadie, B. J., 1978. Satellite observations of calcium carbonate precipitations in the Great Lakes 1. *Limnology and Oceanography*, 23(5), 877-887. DOI: 10.4319/lo.1978.23.5.0877

Vanderploeg, H. A., Eadie, B. J., Liebig, J. R., Tarapchak, S. J., & Glover, R. M., 1987. Contribution of calcite to the particle-size spectrum of Lake Michigan seston and its interactions with the plankton. *Canadian Journal of Fisheries and Aquatic Sciences*, 44(11), 1898-1914. DOI: 10.1139/f87-234

Verpoorter, C., Kutser, T., Seekell, D. A., & Tranvik, L. J., 2014. A global inventory of lakes based on high-resolution satellite imagery. *Geophysical Research Letters*, 41(18), 6396-6402. DOI: 10.1002/2014GL060641

Wiik, E., Bennion, H., Sayer, C. D., & Willby, N. J., 2014. Chemical and biological responses of marl lakes to eutrophication. *Freshwater Reviews*, 6(2), 35-62. DOI: 10.1608/FRJ-6.2.630

Woolway, R. I., Kraemer, B. M., Lenters, J. D., Merchant, C. J., O'Reilly, C. M., & Sharma, S., 2020. Global lake responses to climate change. *Nature Reviews Earth & Environment*, 1-16.

Wunder, S., 2015. Revisiting the concept of payments for environmental services. *Ecological economics*, 117, 234-243. DOI: 10.1016/j.ecolecon.2014.08.016

Preprints (www.preprints.org) | NOT PEER-REVIEWED | Posted: 7 August 2020 doi:10.20944/preprints202008.0192.v1

Annex

Annex 1.

Table A1. Daily maximum and minimum temperature and precipitation data for the year 2015. Underline date indicates image of satellite. * Date whiting phenomenon observed.

Date	Max. Temp	Min. Temp.	Rainfall l/m^2
01/07/2015	34,8	21,2	0
02/07/2015	34,1	20,4	0
03/07/2015	33,3	19,6	0
04/07/2015	36,2	21,1	0
05/07/2015	38,1	23,4	0
06/07/2015	38,4	22,6	0
07/07/2015	38,0	21,1	0
08/07/2015	38,1	19,7	0
09/07/2015	37,1	19,9	0
10/07/2015	36,3	19,4	0
11/07/2015	35,4	17,0	0
12/07/2015	36,1	18,6	0
13/07/2015	37,1	18,4	0
14/07/2015	38,3	20,6	0
15/07/2015	37,8	20,3	0
16/07/2015*	37,7	20,7	0
17/07/2015	36,3	22,2	0
18/07/2015	31,8	21,2	2,0
19/07/2015	33,1	18,8	0
20/07/2015	35,3	18,3	0
21/07/2015	35,9	21,3	0
22/07/2015	33,1	19,9	5,4
23/07/2015	34,6	16,8	0
24/07/2015	34,4	18,7	0
25/07/2015	33,3	18,2	0
26/07/2015	34,9	19,5	0
27/07/2015	36,1	18,0	0
28/07/2015	36,6	19,3	0
29/07/2015	36,2	20,3	0
30/07/2015	33,6	19,4	0
31/07/2015	30,6	19,5	0
01/08/2015	30,5	15,5	3,0
02/08/2015	33,1	18,0	0
03/08/2015	36,0	19,8	0
04/08/2015	34,4	20,2	0
05/08/2015	36,5	19,1	0
06/08/2015	37,7	19,1	0
07/08/2015	34,9	22,3	0
08/08/2015	25,7	19,5	0
09/08/2015	32,5	16,5	0
10/08/2015	34,6	15,1	0
11/08/2015	33,5	19,2	0
12/08/2015	34,4	18,4	0
13/08/2015	27,0	17,5	0
14/08/2015	26,5	13,9	0

Preprints (www.preprints.org) | NOT PEER-REVIEWED | Posted: 7 August 2020 doi:10.20944/preprints202008.0192.v1

Table A2. Daily maximum and minimum temperature and precipitation data for the year 2016. Underline date indicates image of satellite. * Date whiting phenomenon observed.

Date	Max. Temp.	Min. Temp.	Rainfall l/m^2	Date	Max. Temp.	Min. Temp.	Rainfall l/m^2
09/07/2016	34,8	16,2	0	01/08/2016	33,2	15,8	0
10/07/2016	36,2	18,2	0	02/08/2016	35,7	19,1	0
11/07/2016	35,7	21,0	0	03/08/2016	36,0	20,0	0
12/07/2016	32,8	18,0	0	04/08/2016	35,1	18,3	0
13/07/2016	29,7	17,1	0	05/08/2016	33,4	18,8	0
14/07/2016	29,5	12,5	0	06/08/2016	34,7	17,1	0
15/07/2016	30,0	12,2	0	07/08/2016	34,6	17,3	0
16/07/2016	32,6	15,6	0	08/08/2016	34,3	16,4	0
17/07/2016	34,3	15,8	0	09/08/2016*	33,8	16,3	1,8
18/07/2016	35,6	16,3	0	10/08/2016	27,3	16,0	1,0
19/07/2016	36,8	18,7	0	11/08/2016	29,8	13,3	0
20/07/2016	32,4	22,8	0,2	12/08/2016*	30,4	15,8	0
21/07/2016	34,0	20,5	0	13/08/2016	32,7	15,0	0
22/07/2016	32,2	16,1	0	14/08/2016	32,6	15,2	0
23/07/2016	31,4	16,2	0	15/08/2016	32,7	15,9	0
24/07/2016	31,5	17,3	0	16/08/2016	29,1	19,4	0,2
25/07/2016	35,2	17,7	0	17/08/2016	32,2	16,3	0,2
26/07/2016	35,9	18,6	0	18/08/2016	32,5	15,7	0
27/07/2016	35,3	22,1	0,2	19/08/2016*	33,8	16,0	0
28/07/2016	36,0	19,4	0	20/08/2016	31,7	17,2	0
29/07/2016	36,2	20,5	0	21/08/2016	31,7	17,6	0
30/07/2016	34,4	20,6	0	22/08/2016	34,7	17,8	0
31/07/2016	32,4	17,1	0	23/08/2016	35,4	17,9	0

Preprints (www.preprints.org) | NOT PEER-REVIEWED | Posted: 7 August 2020 doi:10.20944/preprints202008.0192.v1

Table A3. Daily maximum and minimum temperature and precipitation data for the year 2017. Underline date indicates image of satellite. * Date whiting phenomenon observed.

Date	Max. Temp.	Min. Temp.	Rainfall l/m^2
01/07/2017	24,8	11,9	0
02/07/2017	30,5	9,5	0
03/07/2017	32,7	13,7	0
04/07/2017	32,5	16,6	0
05/07/2017	33,7	18,8	1,2
06/07/2017	29,7	18,8	1,6
07/07/2017	27,3	13,2	46,0
08/07/2017	24,3	14,0	52,6
09/07/2017	30,5	13,1	0
10/07/2017	32,6	16,9	0
11/07/2017	33,9	17,5	0
12/07/2017	36,5	16,4	0
13/07/2017	39,0	18,4	0
14/07/2017	38,9	21,2	0
15/07/2017	35,5	20,2	0
16/07/2017	34,8	20,2	0
17/07/2017	34,1	21,3	0
18/07/2017	35,2	19,5	0
19/07/2017	32,5	20,3	0
20/07/2017	31,3	16,1	0
21/07/2017	31,0	19,4	0
22/07/2017	32,4	17,0	0
23/07/2017	33,1	17,1	0

Date	Max. Temp.	Min. Temp.	Rainfall l/m^2
24/07/2017	31,5	16,6	0
25/07/2017*	31,0	14,0	0
26/07/2017	32,8	13,9	0
27/07/2017	35,9	17,8	0
28/07/2017*	36,6	18,8	0
29/07/2017	36,3	18,3	0
30/07/2017	36,2	18,7	0
31/07/2017	34,8	20,7	0
01/08/2017	33,0	19,0	0
02/08/2017	31,6	21,0	3,8
03/08/2017	36,3	17,8	0
04/08/2017*	37,9	17,4	0
05/08/2017	38,0	21,0	0
06/08/2017	34,8	20,9	0
07/08/2017	35,9	19,5	0
08/08/2017	30,3	16,5	0
09/08/2017	29,8	14,3	0
10/08/2017	27,0	10,4	0
11/08/2017	29,2	11,0	0
12/08/2017	31,7	13,1	0
13/08/2017	32,0	15,9	0
14/08/2017	33,8	16,4	0
15/08/2017	34,6	20,5	0

Preprints (www.preprints.org) | NOT PEER-REVIEWED | Posted: 7 August 2020 doi:10.20944/preprints202008.0192.v1

393 Table A4. Daily maximum and minimum temperature and precipitation data for the year
394 2018. Underline date indicates image of satellite. * Date whiting phenomenon observed.

Date	Max. Temp.	Min. Temp.	Rainfall l/m^2	Date	Max. Temp.	Min. Temp.	Rainfall l/m^2
01/07/2018	28,0	15,6	0	02/08/2018	37,8	19	0
02/07/2018	28,3	13,1	0	03/08/2018	38,6	19,8	0
03/07/2018	31,5	12,8	0	04/08/2018	37,9	17,6	0
04/07/2018	28,5	15,0	0	05/08/2018	36,6	20,4	0
05/07/2018	28,0	12,1	0	06/08/2018	38,0	21,0	0,2
06/07/2018	30,6	14,0	0	07/08/2018	36,5	20,0	0
07/07/2018	31,9	19,7	0	08/08/2018	34,0	19,9	0
08/07/2018	32,6	18,1	0	09/08/2018	31,2	19,0	0
09/07/2018	33,8	18,8	0	10/08/2018	29,7	17,9	0
10/07/2018	33,2	18,0	0	11/08/2018	32,8	19,4	0
11/07/2018	33,0	18,0	0	12/08/2018	34,3	19,5	2,0
12/07/2018	31,1	17,4	0	13/08/2018	32,5	18,0	0
13/07/2018	32,3	18,7	0	14/08/2018	32,4	16,4	0
14/07/2018	32,1	17,0	0	15/08/2018	32,5	18,8	0
15/07/2018	30,0	14,8	0	16/08/2018	23,5	17,8	2,4
16/07/2018	28,8	15,7	0	17/08/2018	30,6	16,0	0,2
17/07/2018	32,9	15,5	0	18/08/2018	27,7	16,6	0
18/07/2018	32,1	19,4	0	19/08/2018	30,6	15,9	0
19/07/2018	33,1	15,6	0	20/08/2018	31,5	15,1	0
20/07/2018	31,5	14,3	0	21/08/2018	32,2	15,9	4,8
21/07/2018	30,1	14,5	0	22/08/2018*	32,1	15,4	0
22/07/2018	31,1	19,1	0	23/08/2018	32,6	16,0	3,6
23/07/2018	33,8	16,8	0	24/08/2018	32,0	13,2	0
24/07/2018	33,1	16,7	0	25/08/2018	32,0	13,9	0
25/07/2018	35,0	15,6	0	26/08/2018	32,6	16,6	0
26/07/2018	34,5	18,0	0	27/08/2018*	34,6	14,8	0
27/07/2018	34,5	17,0	0	28/08/2018	33,6	19,7	4,6
28/07/2018	33,5	15,4	0	29/08/2018*	31,6	17,2	0
29/07/2018	32,5	14,1	0	30/08/2018	30,3	16,8	0
30/07/2018	34,3	13,9	0	31/08/2018	32,2	18,5	0
31/07/2018	35,4	15,5	0	01/09/2018*	32,1	17,7	3,8
01/08/2018	36,6	20,3	0	02/09/2018	34,2	18,2	0

395
396

Preprints (www.preprints.org) | NOT PEER-REVIEWED | Posted: 7 August 2020 doi:10.20944/preprints202008.0192.v1

Table A5. Daily maximum and minimum temperature and precipitation data for the year 2019. Underline date indicates image of satellite. * Date whiting phenomenon observed.

Date	Max. Temp.	Min. Temp.	Rainfall l/m^2
03/07/2019	33,1	18,5	0,8
04/07/2019	31,8	18,6	0
05/07/2019	33,6	17,9	0
06/07/2019	34,4	16,7	0
07/07/2019	34,3	18,1	0
08/07/2019	31,3	17,3	0
09/07/2019	29,0	14,5	0
10/07/2019	32,1	14,6	0,8
11/07/2019	36,9	17,5	0,8
12/07/2019	39,0	19,2	0
13/07/2019	37,0	23,8	0
14/07/2019	32,1	18,2	0
15/07/2019	33,8	17,5	0
16/07/2019	34,9	20,7	0
17/07/2019	32,9	17,9	0
18/07/2019	34,4	17,5	0
19/07/2019	35,0	19,6	0
20/07/2019	36,7	21,1	0
21/07/2019	35,1	22,5	0
22/07/2019	35,2	20,7	0
23/07/2019	36,0	21,0	0
24/07/2019	36,5	20,6	0

Date	Max. Temp.	Min. Temp.	Rainfall l/m^2
25/07/2019	36,1	22,8	0
26/07/2019	32,0	20,7	0
27/07/2019	27,0	15,3	0
28/07/2019	29,9	12,8	0
29/07/2019	32,4	15,0	0
30/07/2019	33,0	14,5	0
31/07/2019	29,8	17,4	0
01/08/2019	33,6	16,9	0
02/08/2019	35,3	16,9	0
03/08/2019	35,3	19,7	0
04/08/2019	35,5	18,9	0
05/08/2019	36,0	18,3	0
06/08/2019	35,5	18,6	0
07/08/2019	31,8	17,7	0
08/08/2019	33,6	16,3	0
09/08/2019*	33,7	17,7	0
10/08/2019	32,7	18,2	0
11/08/2019	30,9	19,4	0
12/08/2019*	29,2	15,8	0
13/08/2019	29,3	15,9	0
14/08/2019*	32,5	15,2	0

Preprints (www.preprints.org) | NOT PEER-REVIEWED | Posted: 7 August 2020 doi:10.20944/preprints202008.0192.v1

Annex 2.

Lake views before and during the white phenomenon over five years.

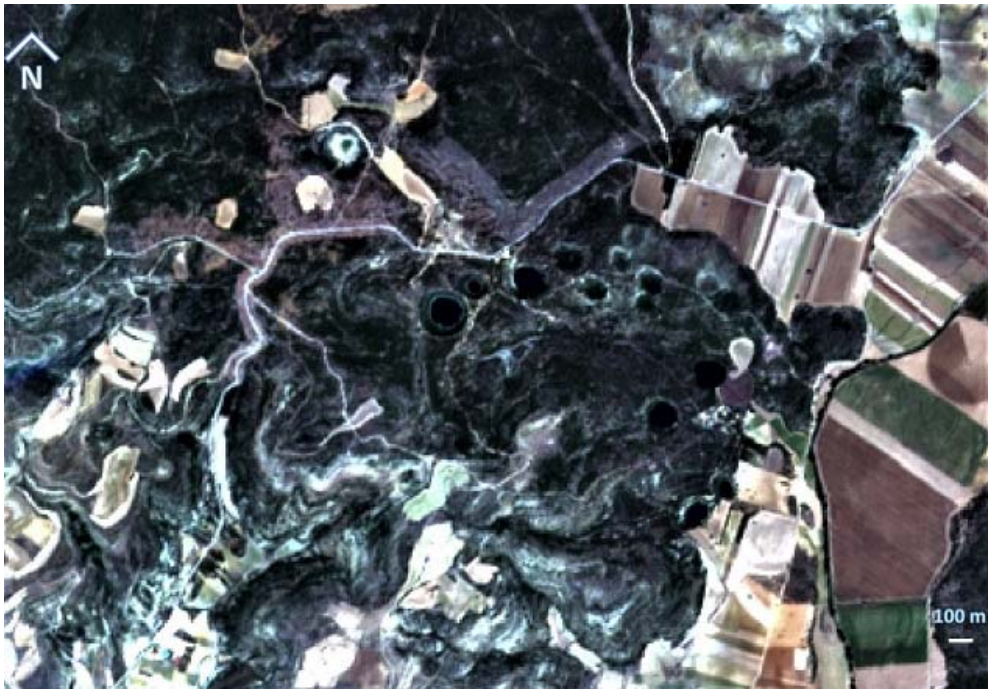

Figure A1. Satellite image in false colour of the Cañada del Hoyo karstic lakes. Up, image on July 06, 2015; the Gitana lake is in its normal state. Down. Image on July 16, 2015; the lake can be seen during the whiting phenomenon in blue cyan.

Preprints (www.preprints.org) | NOT PEER-REVIEWED | Posted: 7 August 2020 doi:10.20944/preprints202008.0192.v1

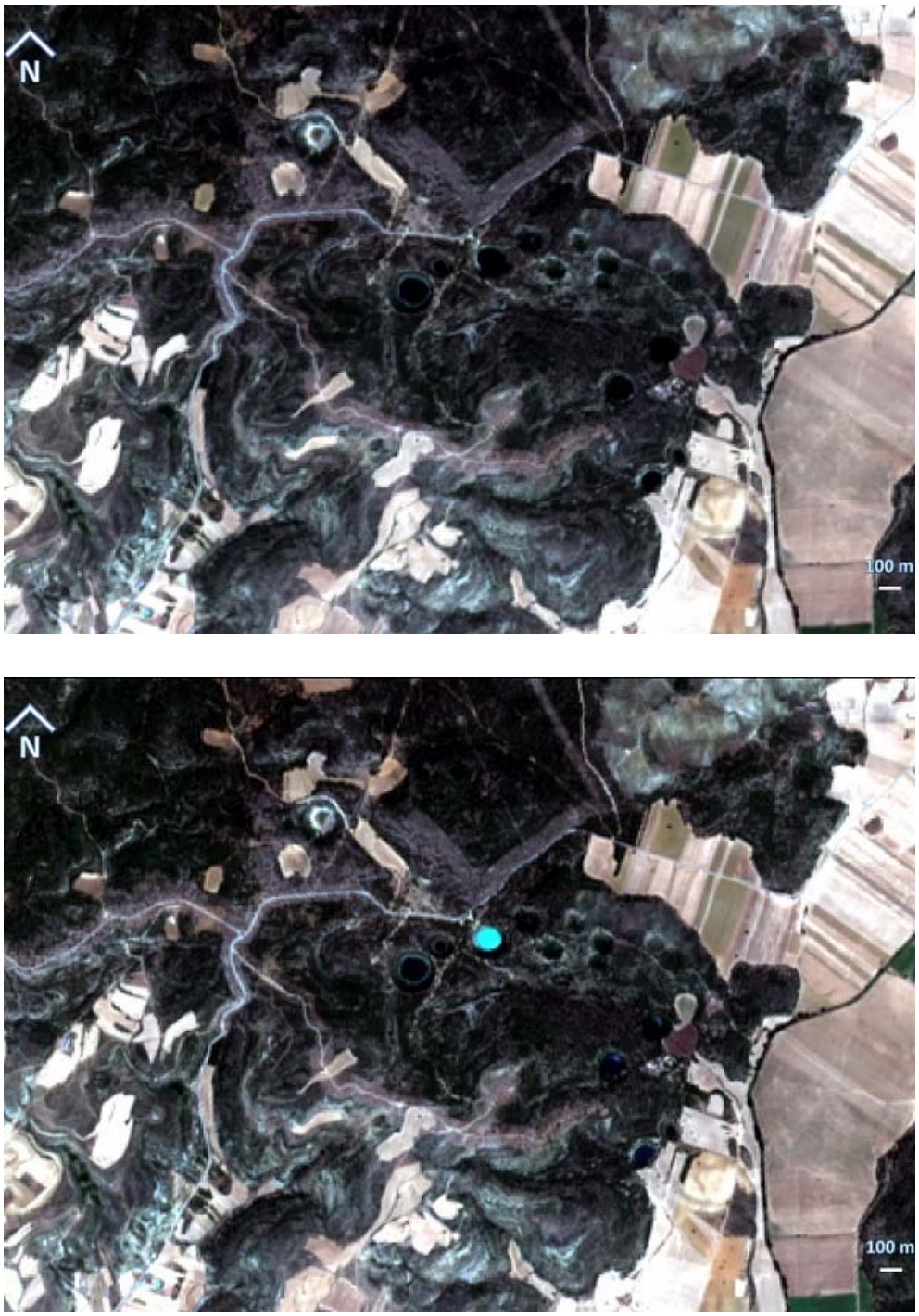

Figure A2. Satellite image in false colour of the Cañada del Hoyo karstic lakes. Up, image on July 30, 2016; the Gitana lake is in its normal state. Down. Image on Aug. 12, 2016; the lake can be seen during the whiting phenomenon in blue cyan.

Preprints (www.preprints.org) | NOT PEER-REVIEWED | Posted: 7 August 2020 doi:10.20944/preprints202008.0192.v1

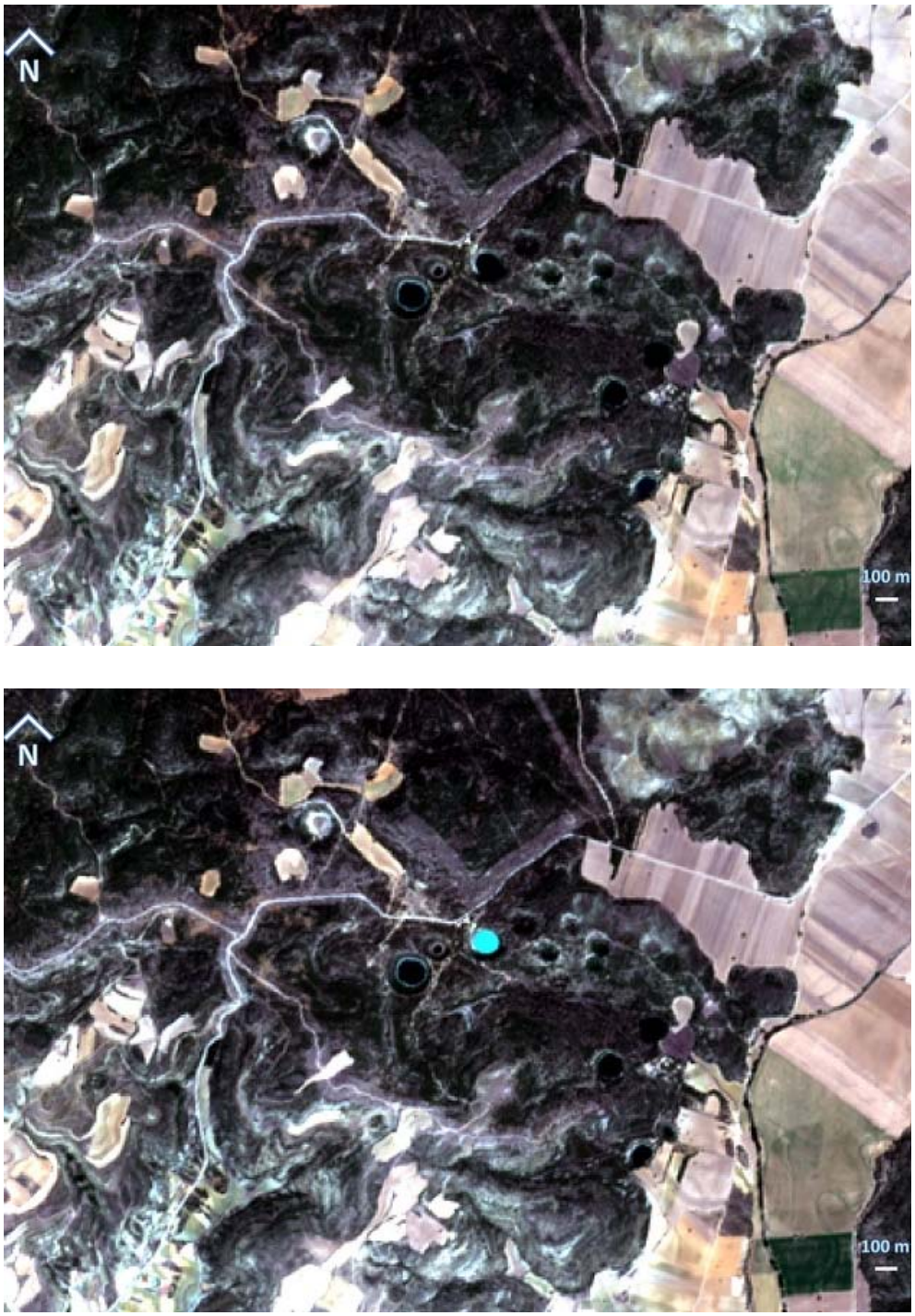

Figure A3. Satellite image in false colour of the Cañada del Hoyo karstic lakes. Up, image on Aug. 14, 2017; the Gitana lake is in its normal state. Down. Image on July 25, 2017; the lake can be seen during the whiting phenomenon in blue cyan.

Preprints (www.preprints.org) | NOT PEER-REVIEWED | Posted: 7 August 2020 doi:10.20944/preprints202008.0192.v1

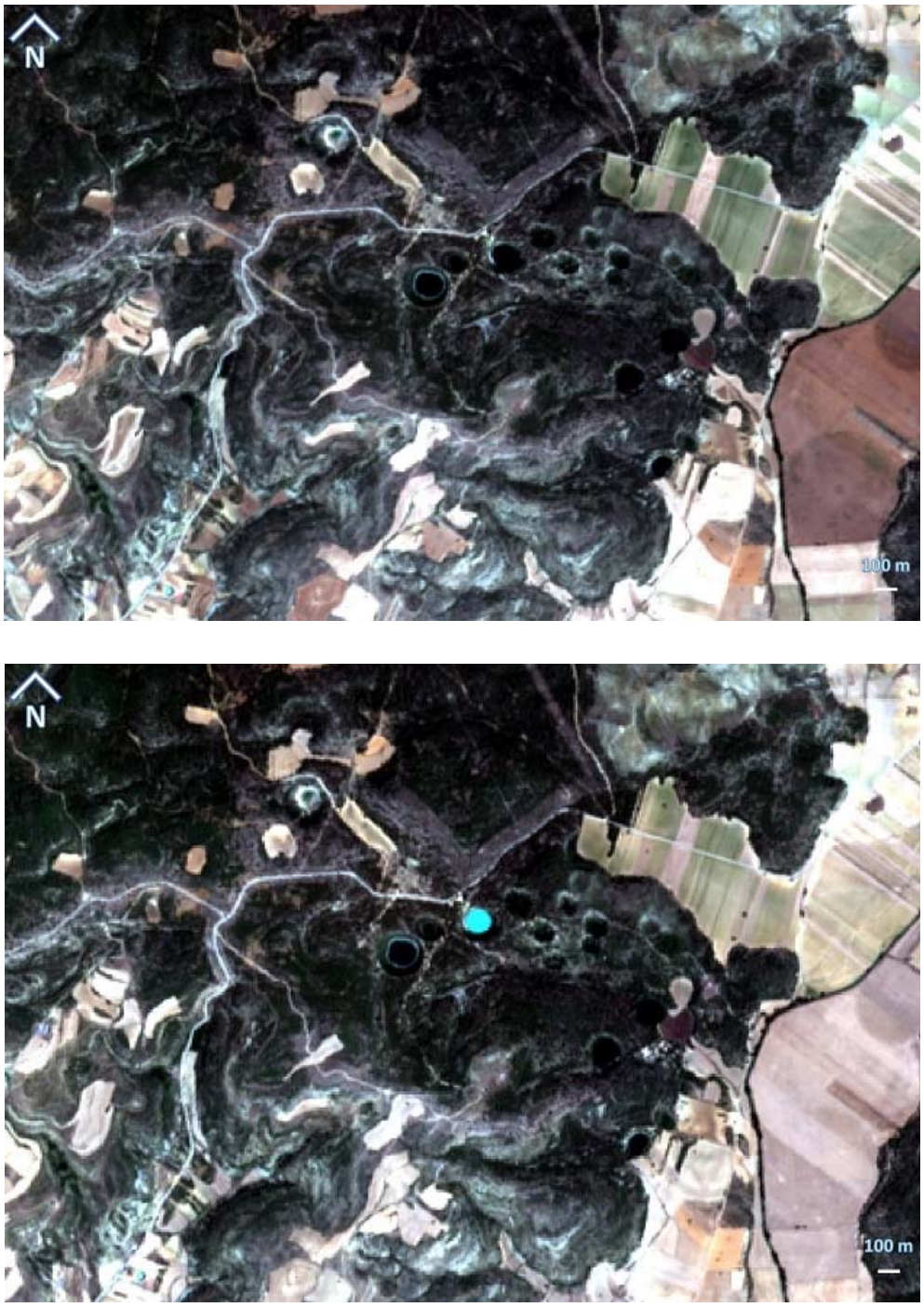

Figure A4. Satellite image in false colour of the Cañada del Hoyo karstic lakes. Up, image on July 20, 2018; the Gitana lake is in its normal state. Down. Image on Aug. 22, 2018; the lake can be seen during the whiting phenomenon in blue cyan.

Preprints (www.preprints.org) | NOT PEER-REVIEWED | Posted: 7 August 2020 doi:10.20944/preprints202008.0192.v1

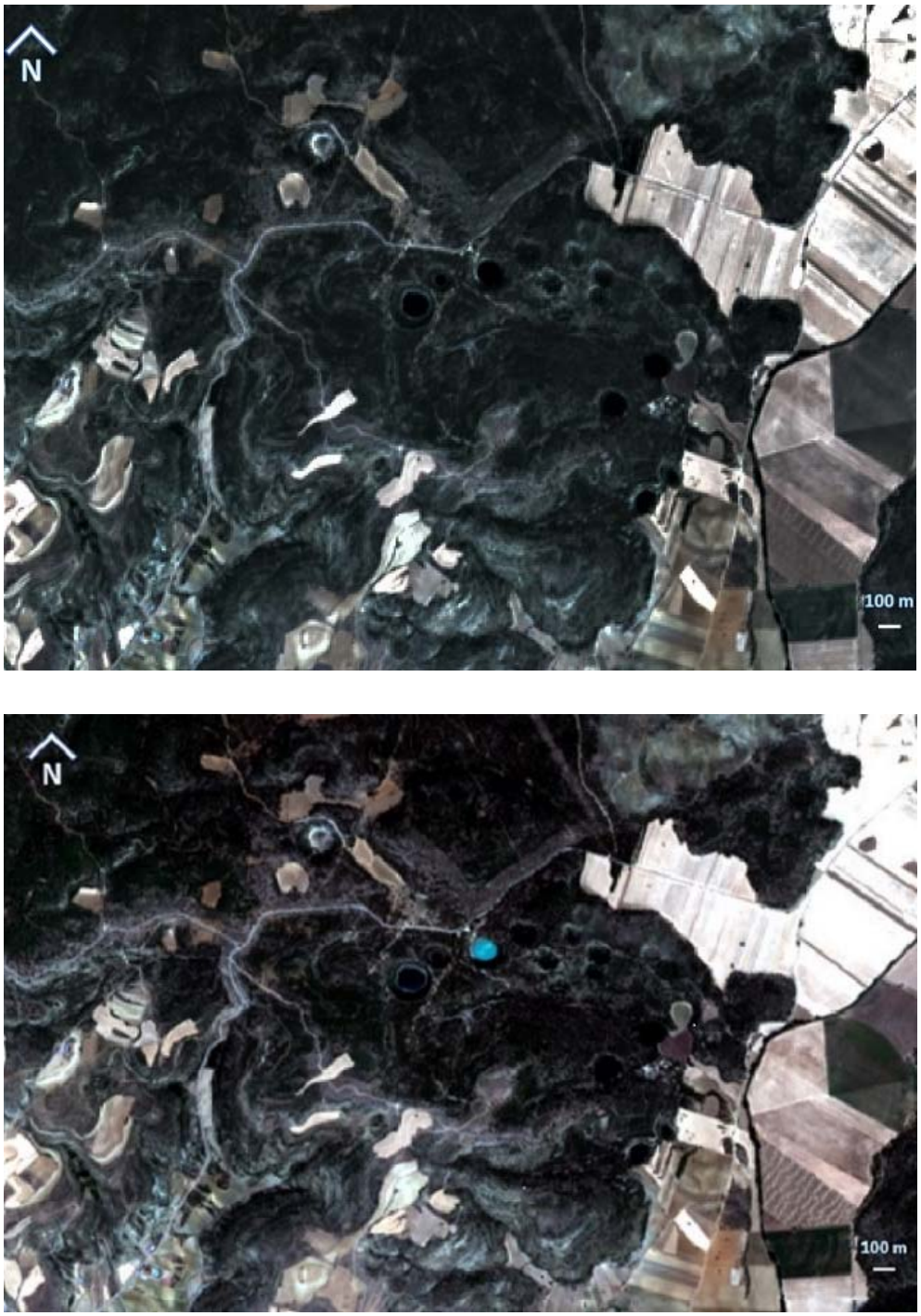

Figure A5. Satellite image in false colour of the Cañada del Hoyo karstic lakes. Up, image on July 25, 2019; the Gitana lake is in its normal state. Down. Image on Aug. 12, 2019; the lake can be seen during the whiting phenomenon in blue cyan.

Preprints (www.preprints.org) | NOT PEER-REVIEWED | Posted: 7 August 2020 doi:10.20944/preprints202008.0192.v1

443